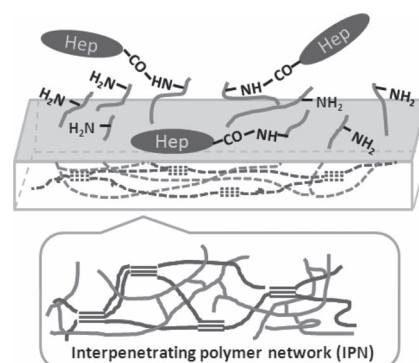


# Surface Engineering of Poly(ethylene terephthalate) for Durable Hemocompatibility via a Surface Interpenetrating Network Technique

Jiang Li, Francis Lin, Lingdong Li, Jing Li, Song Liu\*

Heparin was covalently bonded on chemically inert PET substrate using a surface modification technique—surface interpenetrating network with the purpose of fabricating long-lasting biocompatible materials as vascular grafts. FTIR and XPS spectra confirmed the successful heparinization of PET (PET-Hep). The density of surface-immobilized heparin as quantified by a colorimetric method could reach  $2.4 \mu\text{g cm}^{-2}$  (in the reported optimal range:  $1.5\text{--}3.0 \mu\text{g cm}^{-2}$ ). The hemocompatibility of the heparin-immobilized PET was improved as evidenced by a platelet adhesion test: significantly less platelet adhesion on PET-Hep (11.60%) than on untreated PET (48.91%). An MTT assay indicated PET-Hep was nontoxic to human dermal fibroblast cells. After an initial 5.24% loss of heparin from PET-Hep in the first 14 h immersion in PBS buffer solution, no further leaching of heparin was found.



## 1. Introduction

Cardiovascular diseases (CAD) remain the number one cause of mortality globally and often necessitate surgical intervention with bypass grafts. In the USA, for example, CAD accounted for 33.6% deaths in 2007 and more than 0.6 million victims of atherosclerosis received percutaneous coronary intervention or coronary artery bypass graft.<sup>[1]</sup> It was reported that in comparison with medical therapy

alone, combination of medical therapy with revascularization by coronary artery bypass surgery or percutaneous intervention significantly improves the survival rate of patients with nonacute CADs.<sup>[2]</sup> Generally, surgical bypass is the only option in limb salvage from vascular occlusion. The ideal bypass grafts are autologous vessels harvested from patient's own saphenous vein or internal mammary artery. However, harvesting vessels with sufficient length for effective bypass without causing additional morbidity, can be difficult to achieve in many patients, due to previous surgery or injury.<sup>[3]</sup> Artificial vascular grafts are therefore widely used to replace or bypass diseased arteries.

Polyethylene terephthalate (PET) has become a standard vascular replacement in graft surgeries since 1957<sup>[4]</sup> due to its excellent tensile strength and good chemical resistance.<sup>[5]</sup> After 50 years of development, large-diameter PET vascular grafts ( $>6 \text{ mm}$ ) can remain functioning for more than 10 years while small-diameter PET vascular grafts still fall short in meeting the biological challenges. They may cause blood clots as soon as being implanted because

J. Li, L. Li, Prof. S. Liu

Department of Textile Sciences, Faculty of Human Ecology,  
University of Manitoba, Winnipeg, Manitoba R3T 2N2 (Canada)  
E-mail: liuso@cc.umanitoba.ca

L. Li, Prof. S. Liu

Department of Chemistry, Faculty of Science, University of  
Manitoba, Winnipeg, Manitoba R3T 2N2 (Canada)

Prof. F. Lin, J. Li

Department of Physics & Astronomy, Faculty  
of Science, University of Manitoba, Winnipeg,  
Manitoba R3T 2N2 (Canada)

of the low-flow, high resistance condition.<sup>[6]</sup> Hemocompatible bioactive compounds have been coated or grafted onto the luminal walls of PET vascular grafts to improve their hemocompatibility.<sup>[7–10]</sup> For instance, heparin, a good anticoagulant, has been used to improve the hemocompatibility of stents, vascular grafts, and other biomaterials, which may come into contact with blood.<sup>[11,12]</sup> While many efforts have been directed to covering the surface of PET substrates with heparin, majority of the work focus on physical coating<sup>[9,13,14,15]</sup> with only a few reports on the covalent immobilization of heparin on PET substrates.<sup>[16,17]</sup> Since conventional physical coatings are potentially unstable for long-term applications, it is desirable to create durable covalent linkage between the bioactive agents and the substrate. However, PET is relatively chemically inert. Chemical modification of PET could be quite challenging. To activate PET substrate for the durable immobilization of bioactive agents such as gelatin and heparin, reduction,<sup>[18]</sup> aminolysis,<sup>[19]</sup> hydrolysis,<sup>[20]</sup> nucleophilic substitution of benzene rings in PET backbone with formaldehyde,<sup>[8]</sup> and plasma treatment<sup>[21]</sup> have been studied. Reduction, aminolysis, and hydrolysis can all cause polymeric degradation of PET backbone and removal of the top modified layer, exposing the underneath unmodified PET surface.<sup>[18,19,20,22,23]</sup> This, in turn, negates any modification generated by those processes. Using silane to create bonded layers of silane coating can better preserve the surface structure of PET even though it brings in other issues like uneven coating and only small percentage of free amines for further chemistry (immobilization of bioactive agents).<sup>[18]</sup> The wet chemistry involving formaldehyde suffers from an obvious drawback of using a volatile carcinogen. Surfaces activated by nitrogen and oxygen plasma treatment can reportedly return to their untreated state, called an aging effect.<sup>[24]</sup> A nondestructive, efficient surface modification of PET to achieve durable immobilization of nonthrombogenic bioactive agents is desirably needed.

We reported a surface modification technique for semicrystalline thermoplastic polymers — surface modification by forming an interpenetrating polymer network (IPN).<sup>[25,26,27]</sup> A functional vinyl monomer and a divinyl crosslinker copolymerized in the solvent swollen surface of a semicrystalline polymeric substrate to form an interpenetrating network for durable immobilization of the functional polymer formed in situ. The method has the following advantages: (1) durably immobilizing functional groups onto chemically inert semicrystalline substrates; (2) limiting the modification in a superficial surface without compromising the bulk property of the substrate; (3) introducing versatile functional groups as well as achieving high surface densities of those functional groups. All of these advantages make it a good candidate technique to durably introduce anticoagulants

onto the surface of PET for its long-term use as vascular prostheses.

We have successfully introduced amide and alkynyl groups onto PET using the IPN technique.<sup>[25–27]</sup> However, for the immobilization of heparin, amine or carboxylic acid group should first be introduced to serve as an anchoring group. In this paper, we synthesized a vinyl monomer *tert*-butyl 2-(acrylamido)ethylcarbamate (AEAM-Boc) and attempted the immobilization of AEAM-Boc using the IPN method. After removing the Boc protecting group, amine groups resulted on the surface of PET. Subsequently, heparin was bonded onto the aminized PET using EDC/NHS chemistry. The modification of PET substrate was analyzed and confirmed by Fourier transform infrared (FTIR) and X-ray photoelectron spectroscopy (XPS). The antithrombogenic performance of heparin-bonded PET was monitored using a platelet adhesion test. The long-term use potential of the modified PET sample was also evaluated.

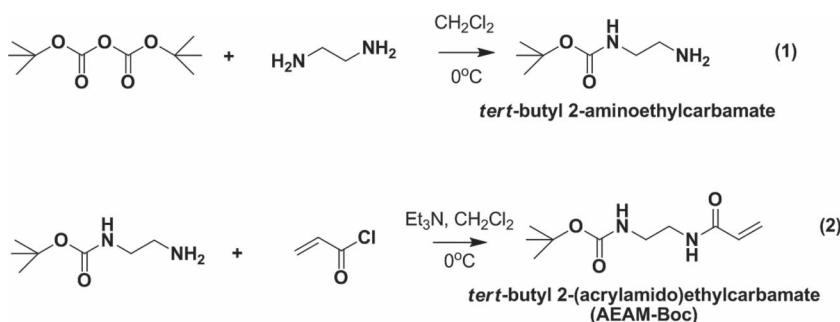
## 2. Experimental Section

### 2.1. Materials and Reagents

Poly(ethylene terephthalate) (PET) plain woven fabric (#777H) was purchased from Testfabrics, Inc. The fabrics were Soxhlet-extracted with distilled (DI) water for 24 h to remove detergents and other impurities. The extracted PET fabrics were then air-dried overnight, stored in a desiccator, and ready for the following experiments. Ethylenediamine (EAM), acryloyl chloride (AC), di-*tert*-butyl dicarbonate (Boc<sub>2</sub>O), Triethylamine (Et<sub>3</sub>N), benzophenone (BP), *N,N'*-methylenebisacrylamide (MBA), *N*-(3-dimethylaminopropyl)-*N'*-ethylcarbodiimide hydrochloride (EDC), *N*-Hydroxysuccinimide (NHS), acid orange 7 (AO), toluidine Blue dye (TB), mepacrine dye, and 3-(4,5-dimethyl-2-thiazolyl)-2,5 diphenyltetrazolium bromide (MTT) were obtained from Sigma–Aldrich (Oakville, ON) and used as received. Human dermal fibroblast cells and fibroblast basal medium were obtained from Cedarlane (Burlington, ON).

### 2.2. Synthesis of *tert*-butyl 2-(acrylamido)ethylcarbamate (AEAM-Boc)

*Tert*-butyl 2-(acrylamido)ethylcarbamate (AEAM-Boc) was synthesized according to a published method.<sup>[28]</sup> One amine group in EAM was protected by *t*-butoxycarbonyl (Boc) before it reacted with AC (Scheme 1). Boc<sub>2</sub>O (32.8 g, 0.15 mol) dissolving in dichloromethane (200 mL) was added to a solution of EAM (40 g, 45 mL, 0.66 mol) at 0 °C drop by drop under stirring reacting for 24 h to obtain *tert*-butyl 2-aminoethylcarbamate [Scheme 1 (1)]. After that, *tert*-butyl 2-aminoethylcarbamate was extracted and dried generating a yield of 21 g (73.61%). AC (11.88 g, 10 mL, 0.1325 mol) dissolving in dichloromethane (100 mL) was added to a solution of *tert*-butyl 2-aminoethylcarbamate (21 g, 0.1325 mol) and Et<sub>3</sub>N (63.6 g, 55 mL, 0.3975 mol) dissolving in dichloromethane (200 mL) at 0 °C drop by drop under stirring reacting for 24 h to obtain AEAM-Boc [Scheme 1 (2)]. Then AEAM-Boc was extracted and solvent was rotary evaporated to remove generating a yield of



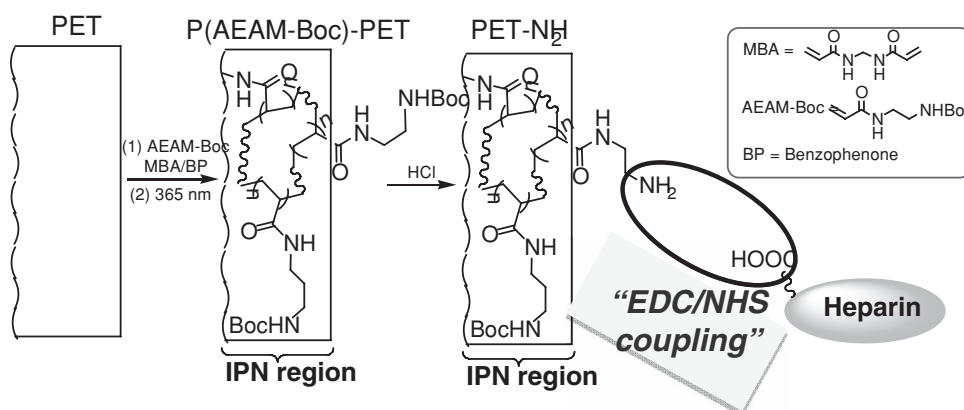
■ Scheme 1. Synthesis of AEAM-Boc.

17 g (60.53%).  $^1\text{H}$  NMR (300 MHz,  $\text{CDCl}_3$ ,  $\delta$ ): 6.23 (d,  $J = 1.35$  Hz, 1H); 6.07–6.16 (m, 1H); 5.64 (dd,  $J_1 = 1.27$  Hz,  $J_2 = 10.08$  Hz, 1H); 3.42–3.47 (m, 2H,  $\text{CH}_2$ ); 3.29–3.35 (m, 2H,  $\text{CH}_2$ ); 1.44 (s, 9H,  $\text{C}(\text{CH}_3)_3$ ).

### 2.3. Immobilization of Poly(AEAM-Boc) onto PET Using the IPN Method

PET fabrics were modified with AEAM-Boc by forming an IPN as previously described.<sup>[25–27]</sup> First, a round PET fabric was swollen in methanol solution containing BP (initiator, 0.55 mol  $\text{L}^{-1}$ ), AEAM-Boc (monomer, 2 mol  $\text{L}^{-1}$ ), and MBA (crosslinker, 1.5% of monomer) at 40 °C for 60 min. Centrifugation (3 min, 3500 rpm) of the swollen specimen was used to remove the excess of solution to achieve a pickup of around 33%. Here, the pickup was calculated as the ratio of the weight of PET fabric after centrifugation to that of untreated PET fabric. The fabric was then exposed under UV irradiation ( $\lambda = 365$  nm, 60 min) to execute a photopolymerization of AEAM-Boc and MBA for the formation of surface IPN. After the polymerization, the sample [named as P(AEAM-Boc)-PET] was extracted with methanol in a Soxhlet-extractor for 24 h, air-dried overnight, and stored in a desiccator for 48 h to obtain a constant weight. The immobilization percentage was calculated according to the following equation:

$$\text{immobilization (\%)} = \frac{W_2 - W_1}{W_1} \times 100\% \quad (1)$$



■ Scheme 2. The scheme of chemical modification of PET samples with heparin.

where  $W_1$  and  $W_2$  are the weights of PET samples before and after the formation of IPN, respectively.

### 2.4. Removal of Boc Protecting Group on P(AEAM-Boc)-PET

P(AEAM-Boc)-PET samples were cut into small pieces, and hydrolyzed in 4 M HCl/1,4-dioxane (ratio = 1:1, v/v) at room temperature to convert NH-Boc groups to amine groups following a previous reported protocol.<sup>[29]</sup> Afterward, the samples were sequentially rinsed with DI water, saturated  $\text{NaHCO}_3$  and DI water to remove excess HCl. The PET sample with amine groups was referred to as PET-NH<sub>2</sub>.

### 2.5. Immobilization of Heparin onto PET-NH<sub>2</sub>

Condensation reaction between carboxylic acid groups of heparin and free amines on PET-NH<sub>2</sub> could result heparinization of PET-NH<sub>2</sub>.<sup>[30]</sup> Carboxylic groups of heparin were activated with EDC and NHS as follows: 1 mg heparin, 1 mg EDC, and 0.6 mg NHS were added into 500  $\mu\text{L}$  citric buffer solution (pH 5.6) at 37 °C for certain time (activation time). The PET-NH<sub>2</sub> samples were then immersed in the above solution of succinimidyl ester of heparin at 37 °C for certain time (reaction time). After the reaction, the heparinized PET samples were shaken in 0.1 M  $\text{Na}_2\text{HPO}_4$  (pH 9.2) for 2 h, followed by sequential washing with 4 M NaCl, and DI water for 24 h, respectively (rinsing solutions were refreshed for at least 4 times in each of the 24 h washing duration). Finally, the modified samples were freeze-dried overnight. The heparin-bonded sample was referred to as PET-Hep.

### 2.6. Instrumental Analysis and Characterization

Proton nuclear magnetic resonance ( $^1\text{H}$  NMR) spectrum of AEAM-Boc was recorded at room temperature in a 5 mm NMR tube on a Bruker Avance 300 MHz NMR spectrometer. Fourier transform infrared (FTIR) spectra of untreated and modified PET samples

were taken on a Nicolet iS10 spectrometer (Thermo Fisher Scientific Inc.) using KBr pellets. X-ray photoelectron spectroscopy (XPS) data of untreated and modified PET samples were acquired with a Kratos Axis Ultra spectrometer by Kratos Analytical, Inc.

## 2.7. Determination of Surface Densities of Amine and Heparin on Modified PET

### 2.7.1. Surface Density of Amine Groups on PET-NH<sub>2</sub>

AO dye was used to determine the surface density of amine groups since amine groups can form 1:1 complex with AO at acidic condition. PET-NH<sub>2</sub> samples (2 × 2 cm<sup>2</sup>) were immersed into 10 mL of AO dye solution (10 mg mL<sup>-1</sup>, pH 3 adjusted by HCl) with constant shaking for 12 h at room temperature. The samples were then rinsed with HCl (pH 3) to remove the residue dye, followed by shaking in NaOH solution (pH 12) for 30 min to extract the specifically adsorbed dye from the samples. The absorbance of dye/NaOH solution was measured at 485 nm.<sup>[31,32]</sup> Afterward, the surface density of amine groups corresponding to dye concentration was then calculated from the calibration curve. The measurement was performed in duplicate.

### 2.7.2. Amount of Heparin Immobilized on PET-Hep

The amount of heparin immobilized on modified PET samples was determined using a colorimetric method.<sup>[32,34]</sup> Three microliters of TB solution (25 mg TB dissolving in 500 mL of 0.01 M HCl containing 0.2% NaCl) was diluted with 2 mL Milli-Q ultrapure water. PET-Hep samples (1 × 1 cm<sup>2</sup>) were then immersed into the solution for 2 h. Five microliters of n-Hexane was added and agitated by a Vortex mixer for 2 min to ensure uniformity of treatment (the same treatment as in constructing a calibration curve even this step is not indispensable in the case of PET-Hep). After removing the PET-Hep-dye complex from the solution, the absorbance of residue aqueous solution was measured at 631 nm and the amount of heparin immobilized on modified PET samples can be calculated from the previously got calibration curve. The measurement was also performed in duplicate.

## 2.8. Stability Test of Immobilized Heparin

To examine the stability of heparin immobilized on the surface of PET substrate, stability test was conducted according to Kang et al.<sup>[34]</sup> and Yang et al.<sup>[35]</sup> PET-Hep samples (1 × 1 cm<sup>2</sup>) were immersed in a big beaker containing PBS (pH 7.4, 50 mL) at room temperature for 1 d. Two pieces of PET-Hep samples were taken out at predetermined times (*t* = 4.8, 9.6, 14.4, 19.2, and 24 h) and the amount of heparin remained on those samples were determined using the colorimetric method. The release of heparin can be calculated as the following equation:

$$\text{Release of heparin(\%)} = \frac{D_1 - D_2}{D_1} \times 100\% \quad (2)$$

where D<sub>1</sub> and D<sub>2</sub> are the surface densities of heparin on PET-Hep samples before and after extraction with PBS solution, respectively.

## 2.9. Biological Tests

### 2.9.1. Platelet Adhesion Test

Platelet adhesion test was carried out in a static blood environment according to the literature.<sup>[36]</sup> Human whole blood was collected from healthy volunteers and mixed with 3.8% sodium citrate solution (ratio of human whole blood and aqueous solution = 9:1, v/v) as an anticoagulant. The blood was centrifuged at 1200 rpm for 15 min at room temperature to obtain platelet-rich plasma (PRP). The number of platelets was determined using a hemocytometer. The platelet concentration of PRP solution was adjusted to 1 × 10<sup>5</sup> cells per microliter by adding phosphate-buffered saline (PBS, pH 7.4) to PRP. The modified (PET-Hep) and untreated PET samples (1 × 1 cm<sup>2</sup>) were equilibrated with PBS (pre-warmed at 37 °C) for 1 h and then immersed into 1 mL of the platelet suspension mentioned above for 2 h at 37 °C with 5% CO<sub>2</sub>. After the incubation, the samples were taken out and gently washed with PBS for three times to remove the nonadhered platelets. The platelets remaining in both PRP solution and the rinsing solution were quantified using the hemocytometer. The extent of platelet adhesion in respect to the PRP control was calculated according to the following equation:

$$\text{Platelet adhesion(\%)} = \frac{P_1 - P_2}{P_1} \times 100 \quad (3)$$

where P<sub>1</sub> is the platelet count in PRP solution before contact and P<sub>2</sub> is the total count of platelet in both PRP solution after contact and the rinsing solution.

Analysis of variance (t-test; *n* = 5) of the results was performed with regard to control (untreated PET) at *p* < 0.05, *p* < 0.01, and *p* < 0.001 of significant level.

The distribution of platelets adhered on those PET samples and the morphology of adhered platelets were observed using an OLYMPUS BX60 fluorescent microscope and a JEOL 840 analytical scanning electron microscope (SEM), respectively. After being removed from the PRP solution, the PET samples were washed with PBS and fixed with 2.5% glutaraldehyde solution (Sigma) for 20 min at room temperature. The samples were washed with PBS again and dehydrated in a series of ethanol/DI water solutions (50, 60, 70, 80, 90, and 100%). Finally, a portion of the PET samples was stained in 10 × 10<sup>-3</sup> M mepacrine solution for 90 min at room temperature and the fluorescent images of platelets on those samples were taken under the fluorescent microscope.<sup>[37]</sup> Another portion of the PET samples was coated with gold in vacuum for SEM observation.

### 2.9.2. Cytotoxicity Test

The cytotoxicity of PET-Hep was evaluated using the MTT assay in human dermal fibroblast cells (PCS 201-010, ATCC). The cells were cultured on T-25 flask with fibroblast basal medium supplemented with fibroblast serum free media. Culture was kept in an incubator at 37 °C with 5% CO<sub>2</sub> and the medium was changed every 3 d. When the cells grew to 80% of confluence, those cells were detached by adding 1 mL of EDTA and 1 mL of Trypsin. The number of cells was determined by a hemocytometer and the



cell concentration of cell suspension can be adjusted by diluting with the culture medium.

The MTT assay is a standard test to determine the viability of cells. The mechanism is that cellular enzymes can reduce yellow MTT (3-(4,5-dimethyl-2-thiazolyl)-2,5-diphenyltetrazolium bromide) to purple formazan crystal. To determine the toxicity of extracts from modified and untreated PET samples, MTT assay was performed as described.<sup>[38]</sup> The samples were equilibrated with PBS for 1 h and immersed in 2 mL of fresh culture medium for 1, 2, and 4 d, respectively. The culture medium was changed every day and preserved. The fibroblast cells were seeded in a sterile 96-well tissue culture plate with a density of  $1.5 \times 10^5$  cells per milliliter using fresh culture medium. After 24 h of incubation, the fresh culture medium was replaced by the medium got at the 1st, 2nd, and the 4th day of extraction for another 24 h incubation at 37 °C with 5% CO<sub>2</sub>. Subsequently, 10  $\mu$ L of MTT solution (dissolved in PBS; 5 mg mL<sup>-1</sup>) was added to each well and the well was incubated for 4 h at 37 °C with 5% CO<sub>2</sub>. After the formation of purple crystals, excess medium and MTT were removed and 100  $\mu$ L of dimethyl sulfoxide was added to each well. The well plate was kept in the same incubator for 10 min to dissolve the crystals. The absorbance of the mixed solution was measured at 560 nm using an Opsys MR™ microplate reader (DYNEX Technologies).

The cell viability was calculated according to the following equation:

$$\text{Cell viability (\%)} = \frac{D_s - D_b}{D_c - D_b} \times 100\% \quad (4)$$

where  $D_s$ ,  $D_b$ , and  $D_c$  are the optical densities of formazan crystals produced by sample, blank (medium without cells) and control (medium with cells), respectively.

Analysis of variance (t-test;  $n = 3$ ) of the results was performed with regard to control (untreated PET) at  $p < 0.05$  and  $p < 0.01$  of significant level.

### 3. Results and Discussion

#### 3.1. Surface Modification and Characterization of PET

The functional monomer AEAM-Boc was synthesized in 2 steps as shown in Scheme 1 and its NMR spectrum (Figure S1, Supporting Information) was identical to that reported in literature.<sup>[28]</sup>

AEAM-Boc was immobilized onto PET using the nondestructive IPN method with an immobilization percentage of 7%. FTIR spectra revealed the successful immobilization given the new peaks at 1697 and 1654 cm<sup>-1</sup> characteristic of AEAM-Boc amide, which are obvious in the subtracted spectrum (Figure 1C). P(AEAM-Boc)-PET was then hydrolyzed

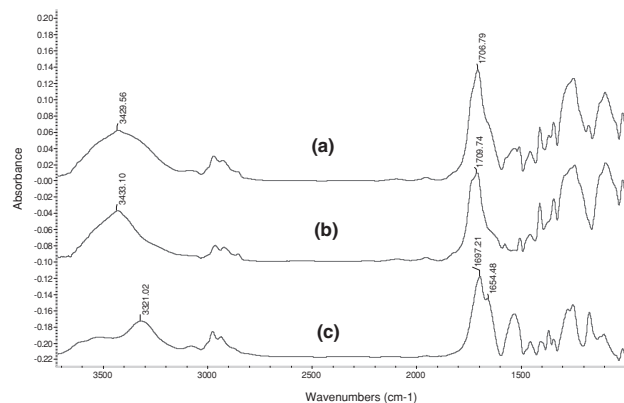


Figure 1. FTIR spectra of (a) PET modified by AEAM-Boc through IPN method (b) Untreated PET (c) subtraction between PET modified by AEAM-Boc and untreated PET.

in 4 M HCl solution to generate free amine groups for further functionalized with heparin. The amounts of amine groups on PET samples were determined using a colorimetric assay. As shown in Figure 2a, surface amine group increased almost linearly with the duration of hydrolysis within the studied hydrolysis period (1–5 h). The depth of color on the samples was also consistent with the titration results: the higher the surface density of amine groups, the more AO deposited onto the substrate by forming 1:1 complex with free amine and the deeper the color (Figure 2b). After the first hour of hydrolysis, the heterogeneous hydrolysis proceeded as a pseudo first-order reaction in the presence of excess amount of HCl. However, the fabric structure of PET substrate could be compromised when hydrolysis time was more than 2 h and even macroscopic damage was visualized after 5 h hydrolysis in 4 M HCl. To effect the covalent bonding of heparin for full coverage on surfaces, the surface density of anchoring amine group is generally in the range

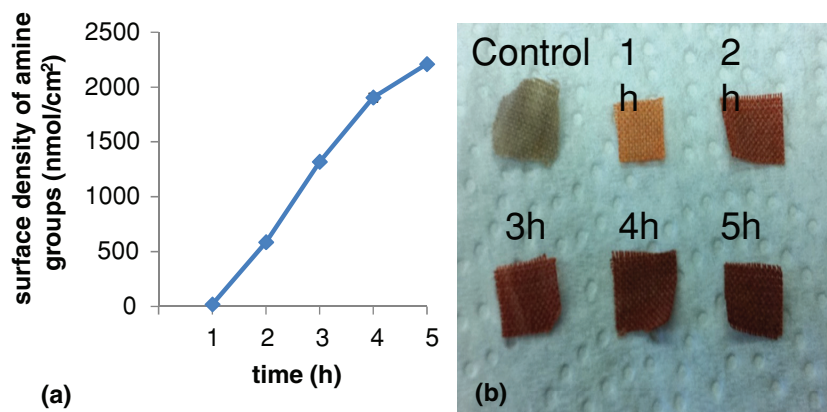


Figure 2. (a) The relationship between the surface density of amine groups generated by hydrolyzing P(AEAM-Boc)-PET and different hydrolysis periods; (b) images of samples dyed with AO.

of 10 to 400 nmol cm<sup>-2</sup>.<sup>[35,39,40]</sup> The surface amine density reached 586.7 nmol cm<sup>-2</sup> after 2 h hydrolysis, which is higher than the high end of the above range (400 nmol cm<sup>-2</sup>) and may be sufficient for the bonding of heparin considering that the bulky heparin may cover up certain amount of amine underneath negating the need of very high density of amine groups. So, PET-NH<sub>2</sub> got from 2 h hydrolysis of P(AEAM-Boc)-PET was used for the following heparin immobilization and characterization.

XPS spectra of PET-NH<sub>2</sub>, PET-Hep, and untreated PET are listed in Figure 3. Compared with the spectrum of untreated PET, a new N 1s peak at 399.55 eV appeared in that of PET-NH<sub>2</sub>, lending support to the successful

immobilization of P(AEAM-Boc) on PET. From the high-resolution N 1s spectrum (inset in Figure 3, **PET-NH<sub>2</sub>**), two different N peaks could be seen indicating the existence of two different forms of N in PET-NH<sub>2</sub>. Carbamate (Boc-protected NH<sub>2</sub>) and amide N corresponded to the peak at 399.53 eV and the another peak at 401.35 eV was from free NH<sub>2</sub> generated from the removal of the protective functional group Boc. According to atomic concentration (%) in XPS data, the conversion ratio from Boc protected NH<sub>2</sub> to free NH<sub>2</sub> (top most layers detectable in XPS) can be calculated as 48.1%.

The formation of amide bonding between heparin and PET-NH<sub>2</sub> was facilitated by activating the carboxylic acid

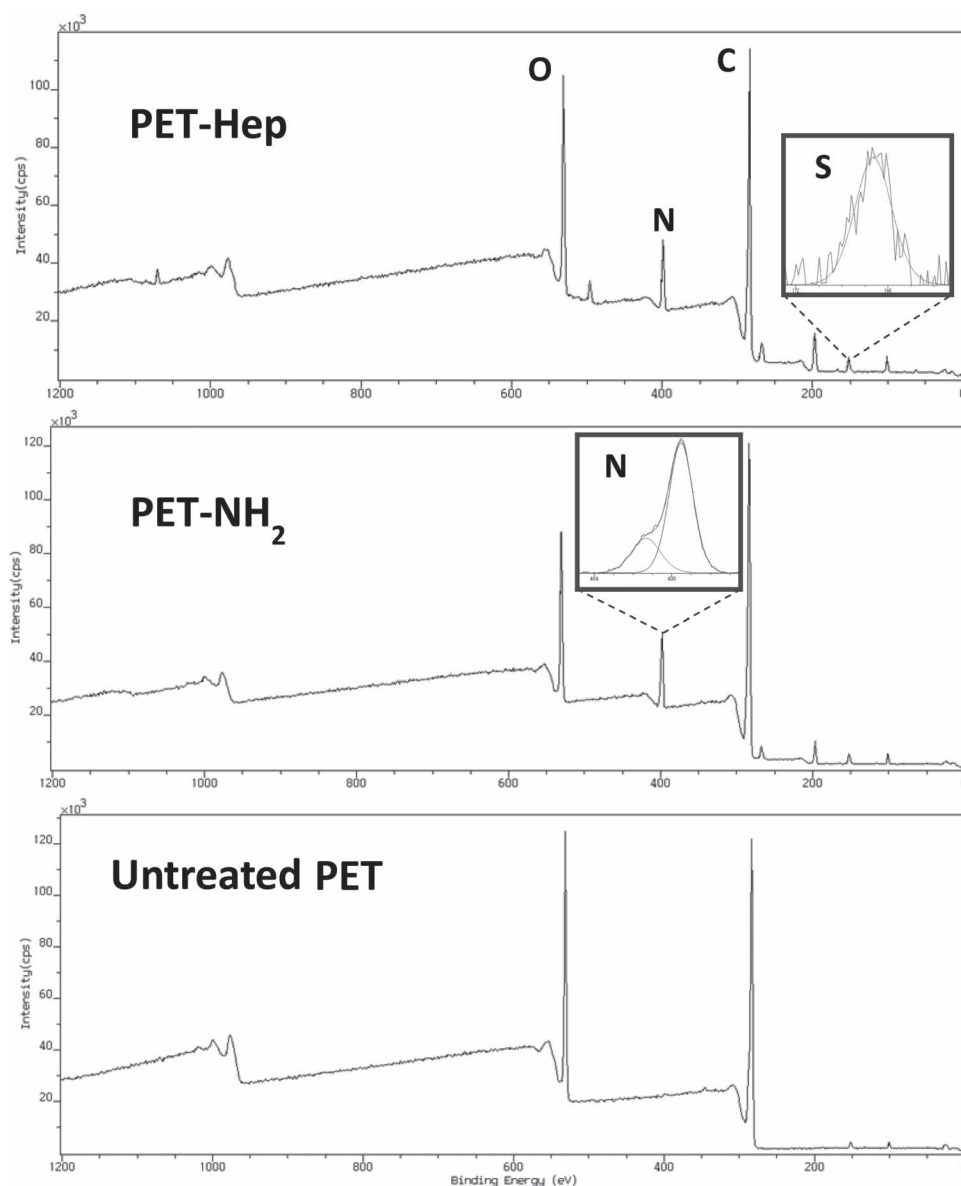


Figure 3. XPS spectra of PET samples (from top to bottom: PET-Hep; PET- NH<sub>2</sub> got from 2 h hydrolysis of P(AEAM-Boc)-PET and untreated PET).

■ Table 1. Surface densities of heparin on PET-Hep.

PET-Hep Samples (activation time + reaction time)	10 min + 4 h	10 min + 24 h	2 h + 24 h
Surface density of heparin [ $\mu\text{g cm}^{-2}$ ]	$0.93 \pm 0.20$	$1.54 \pm 0.20$	$2.40 \pm 0.10$

groups of heparin with NHS and EDC. Both activation and reaction periods affected the amount of heparin bonded onto PET-NH<sub>2</sub>. As shown in Table 1, extended activation (2 h) and reaction (24 h) durations led to higher surface density of heparin ( $2.40 \mu\text{g cm}^{-2}$ ). The reaction time was not further extended since it was reported that heterogeneous heparinization of aminized surfaces reached a plateau after 20–24 h of reaction.<sup>[40]</sup> In addition,  $2.40 \mu\text{g}$  heparin per  $\text{cm}^2$  falls in the reported optimal surface density of heparin for stenosis prevention ( $1.5\text{--}3 \mu\text{g}$  heparin per  $\text{cm}^2$ ).<sup>[41]</sup>  $2.40 \mu\text{g}$  heparin/ $\text{cm}^2$  can be converted to  $4.05 \text{ nmol}$  repeating units per  $\text{cm}^2$  (the repeating unit of heparin C<sub>12</sub>H<sub>19</sub>NO<sub>20</sub>S<sub>3</sub> has a molecular weight (MW) of  $593 \text{ g mol}^{-1}$ ). Hence, the conversion yield from free NH<sub>2</sub> ( $586.7 \text{ nmol cm}^{-2}$ ) to heparin repeating unit can be calculated as  $4.05/586.7 = 0.69\%$ . The reason for the low conversion ratio is manifold. First, heterogeneous reactions always present extremely low yield due to less chance of molecular collision hence reaction. Second, the bulky heparin molecule, once bonded onto the surface through one amide bond from one of its more than 20 repeating units, hinders the approaching of other heparin molecules to the unreacted free amine groups in close vicinity.

After the immobilization of heparin, the N/C (mol%) derived from XPS measurements decreased from 13.27% for PET-NH<sub>2</sub> to 11.59% (Table 2). This drop can be explained by the immobilization of heparin. Since the surface of PET-NH<sub>2</sub> was covered by heparin the N/C of which (8.3%) is lower as compared with 13.27% on the surface of PET-NH<sub>2</sub>. The mole percent of sulfur element on the surface of PET-Hep was almost four times that of the background signal (0.06% on the surface of untreated PET), indicating a successful bonding of heparin on the PET substrate. The high resolution of S 2p spectrum is shown in Figure 3 (PET-Hep) as an inset.

Based on S/N (Table 2), we can also get the conversion percentage as follows:

Suppose  $x$  percent of free amine catches one heparin repeating unit (realistically, it is not the case since once a repeating unit is caught, the whole chain is immobilized. However, for the purpose of comparing with the colorimetric quantification data, we can use the MW of the repeating unit since the final results are based on the same denominator in both cases), then  $S/N = 3x/(2+x) = 0.23/8.76$ ,  $x$  can be solved from the equation as 1.76%. This number is around 2.55 times of the conversion yield (0.69%) derived from the colorimetric quantification data. It is because XPS detects all the heparin molecules sitting on the topmost layer and not all the nitrogen atoms shielded by heparin, the underestimated denominator results a relatively higher estimation of conversion yield.

### 3.2. Biological Evaluation of PET-Hep

Platelet adhesion is an early sign of blood clotting cascade. Thus, platelet adhesion test has been widely adopted to evaluate the hemocompatibility of blood contacting medical devices. Plasma suspension containing platelets was first brought in close contact with test samples for certain time, and platelet adhesion on the samples was then quantified. The antithrombogenic performance partly depends on the platelet adhesion ratio: during a predetermined period, the more platelets adhere on the sample, the worse the sample performs while in contact with blood. Surface modification can be an effective way to improve the hemocompatibility of substrates by avoiding activation and aggregation of platelets. In our case, untreated PET and heparin modified PET samples were immersed in PRP suspension for 2 h. As shown in Figure 4B, platelet adhesion on untreated PET samples reached almost 50%. It is similar to commercial Dacron vascular grafts.<sup>[38]</sup> As a highly sulfated glycosaminoglycan, heparin can effectively form a complex with heparin-binding proteins such as antithrombin III.<sup>[42]</sup> The formed heparin-protein complex

■ Table 2. Surface atomic concentrations (%) of PET samples measured by XPS.

Samples	Atomic concentration [%]				N/C [%]	S/N [%]
	C 1s	N 1s	S 2p	O 1s		
Untreated PET	77.83	0.26	0.06	21.85	0.34	—
PET-NH <sub>2</sub>	75.13	9.97	0.05	14.85	13.27	—
PET-Hep	75.58	8.76	0.23	15.43	11.59	2.63

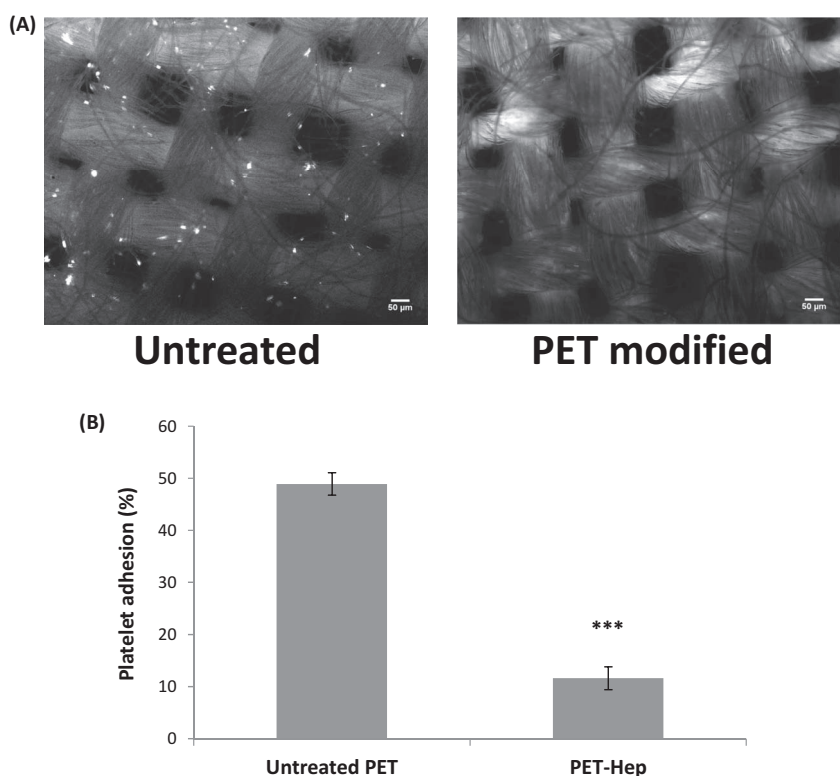


**Figure 4.** (A) Fluorescence images of platelets on untreated PET sample (left) and PET-Hep sample (right) at  $\times 260$  magnification. Platelets were labeled by Mepacrine dye; (B) Quantification of platelet adhesion on control (untreated) and modified (PET-Hep) samples. The diagram includes *t*-test results ( $n = 5$ ) with respect to untreated PET (\* $p < 0.05$  and \*\* $p < 0.01$ ).

nearly a quarter of platelets adhered on untreated PET samples. It is in accordance with the anticoagulation feature of heparin. On the other hand, the result indicates that heparin has been effectively immobilized onto PET substrate with well retained bioactivity using the IPN surface modification technique.

To observe the distribution of platelets adhering on modified and untreated PET samples, platelets were labeled with mepacrine dye. Fluorescence images were taken and shown in Figure 4A. There were significantly more platelets on the surface of untreated PET than the modified PET even though the distribution of platelets was not so uniform. Those images agree with the quantification results of platelet adhesion.

The morphology of modified and untreated PET samples after incubation in platelet suspension was further investigated by SEM. As shown in Figure 5, untreated PET was covered by platelets, which is consistent with the observation of adhered platelets under fluorescent microscope. Signs of pseudopodia could even be observed on the untreated PET (Figure 5b and c), suggesting that some of the adhered platelets have been activated. Again, platelets could hardly be

can further bind with thrombin and prevent thrombin from catalyzing the formation of fibrin network. Platelet adhesion on PET-Hep samples was only 11.60% (Figure 4B),

spotted on the surface of PET-Hep.

After being cultured in the extraction of PET-Hep, the biological response of fibroblast cells was evaluated using

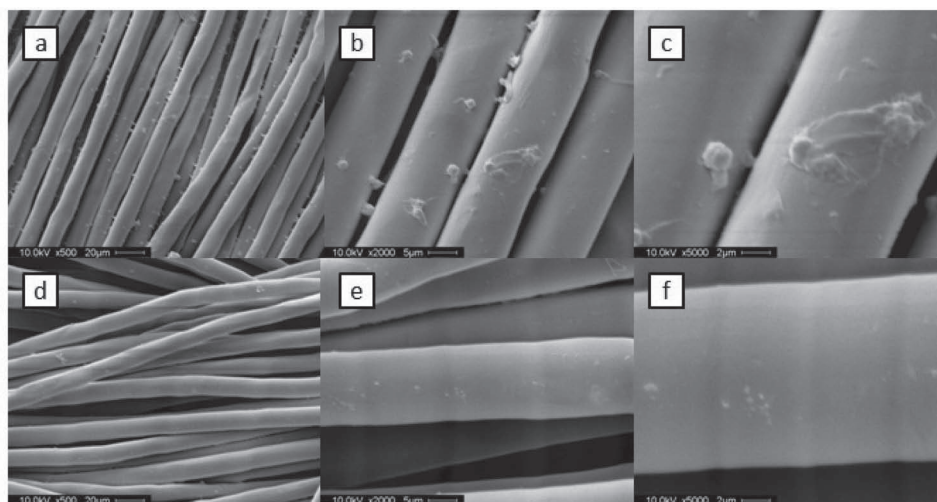


**Figure 5.** SEM images of platelet adhesion after 2 h of incubation on (a) untreated PET sample at  $\times 500$  magnification (b) untreated PET sample at  $\times 2000$  magnification (c) untreated PET sample at  $\times 5000$  magnification (d) PET modified with heparin sample at  $\times 500$  magnification (e) PET modified with heparin sample at  $\times 2000$  magnification (f) PET modified with heparin sample at  $\times 5000$  magnification.



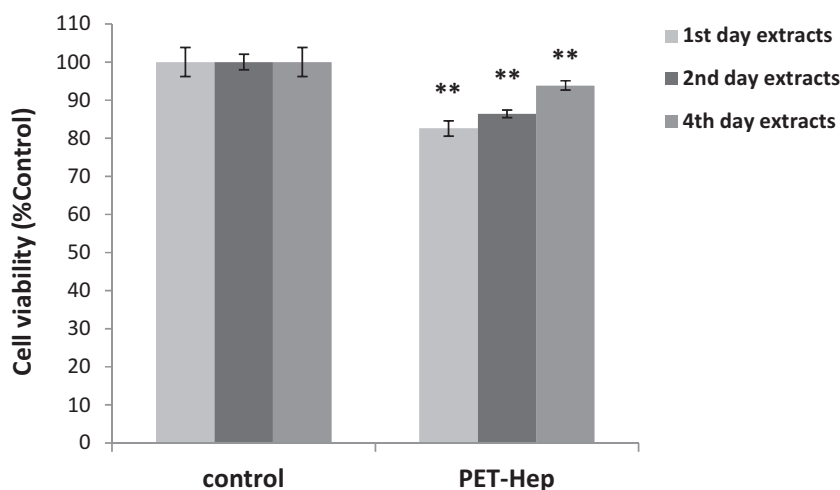


Figure 6. MTT assay for fibroblast cells cultured in control (cell medium) and in the medium with extracts from PET-Hep sample. The diagram includes t-test results ( $n = 3$ ) with respect to control (\* $p < 0.05$  and \*\* $p < 0.01$ ).

the MTT assay. As shown in Figure 6, the relative cell viability in PET-Hep extracts was higher than 80%, indicating that the PET-Hep extracts are not toxic to the cells.<sup>[38]</sup> Ke et al.<sup>[43]</sup> studied the cytotoxicity of AEAM-Boc on HEK293 cells and observed 80% cell viability in the presence of AEAM-Boc at a concentration as high as  $20 \mu\text{g mL}^{-1}$ .<sup>[43]</sup> Since polymer of AEAM-Boc is durably immobilized and covered with biocompatible heparin molecules in the case of PET-Hep, low cytotoxicity of PET-Hep extract is as expected.

### 3.3. Stability of Immobilized Heparin on PET-Hep

To examine the stability of immobilized heparin, PET-Hep samples were immersed into PBS (pH 7.4) solution for

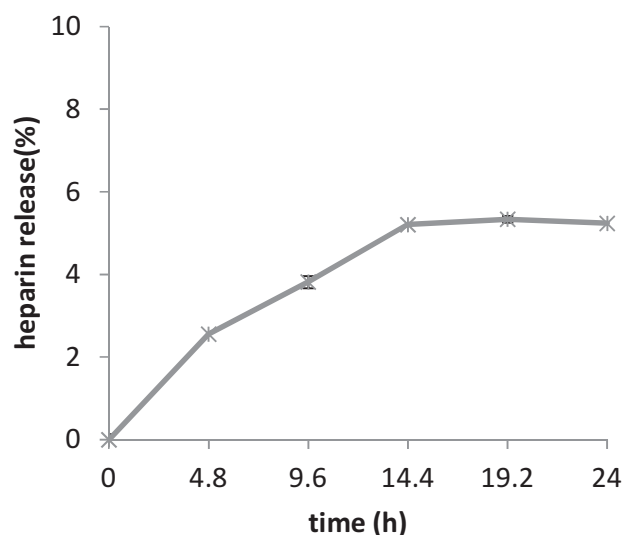


Figure 7. Stability of heparin immobilized on PET-Hep samples.

1 d (24 h). Two pieces of those samples were removed from PBS solution every few hours (4.8 h) and the remaining heparin was quantified by TB O dye titration. The percentage of released heparin increased gradually with the immersion duration and the release curve plateaued at around 5% after 14.4 h (Figure 7). The small portion of heparin loss was probably due to unremoved physically adsorbed heparin on PET-Hep. The fact that more than 94% of heparin immobilized on PET-Hep could sustain 24 h extraction in PBS solution is due to the covalent nature of the bonding between heparin and PET substrate. The finding accords with the previous reported durability of heparin grafted on polyurethane films.<sup>[44]</sup> The bioactive and durable PET-Hep possesses the potential to be used as

vascular grafts, and further research is needed to validate its used in small-diameter vascular prosthesis.

## 4. Conclusion

Durable heparinization of PET (PET-Hep) was achieved by using a surface IPN technique. A vinyl functional monomer AEAM-Boc was polymerized and crosslinked in the swollen surface of PET to form a durable IPN so to anchor amine functional groups onto chemically inert PET allowing the introduction of heparin on the surface through covalent bonding. The formed PET-Hep presented significantly less platelet adhesion with respect to untreated PET (around ¼) and was also nontoxic to the tested fibroblast cells. Because of the covalent nature of heparin bonding on PET substrates, more than 94% of immobilized heparin could sustain 24 h extraction in PBS solution. The heparin engineered PET substrate holds the potential to be used in small-diameter vascular grafts.

## Supporting Information

Supporting Information is available from the Wiley Online Library or from the author.

**Acknowledgements:** The authors are grateful for the financial support from the Natural Sciences and Engineering Research Council of Canada (NSERC) Discovery grant (Grant no.: RGPIN/372048-2009), and the Manitoba Health Research Council (MHRC) Establishment grant.

Received: May 8, 2012; Revised: July 31, 2012; Published online: September 7, 2012; DOI: 10.1002/macp.201200251

Keywords: biocompatibility; heparin; interpenetrating networks; photo-initiated radical polymerization; polyester

- [1] V. L. Roger, A. S. Go, D. M. Lloyd-Jones, R. J. Adams, J. D. Berry, T. M. Brown, M. R. Carnethon, S. F. Dai, G. De Simone, E. S. Ford, C. S. Fox, H. J. Fullerton, C. Gillespie, K. J. Greenlund, S. M. Hailpern, J. A. Heit, H. P. Michael, V. J. Howard, B. M. Kissela, S. J. Kittner, D. T. Lackland, J. H. Lichtman, L. D. Lisabeth, D. M. Makuc, G. M. Marcus, A. Marelli, D. B. Matchar, M. M. Mcdermott, J. B. Meigs, G. S. Moy, D. Mozaffarian, M. E. Mussolino, G. Nichol, N. P. Paynter, W. D. Rosamond, P. D. Sorlie, R. S. Stafford, T. N. Turan, M. B. Turner, N. D. Wong, J. Wylie-Rosett, *Circulation* **2011**, 123, e18.
- [2] A. Jeremias, S. Kaul, T. Rosengart, L. Gruberg, D. Brown, *Am. J. Med.* **2009**, 122, 152.
- [3] A. Thomas, G. R. Campbell, J. H. Campbell, *Cardiovasc. Pathol.* **2003**, 12, 271.
- [4] D. E. Szilagyi, L. C. France, R. F. Smith, J. G. Whitcomb, *Arch. Surg.* **1958**, 77, 538.
- [5] S. Rajendran, S. C. Anand, *Tex. Program* **2002**, 32, 1.
- [6] G. W. Bos, A. A. Poot, T. Beugeling, W. G. Aken, J. Feijen, *Arch. Physiol. Biochem.* **1998**, 106, 100.
- [7] M. J. Moreno, A. Ajji, D. Mohebbi-Kalhor, M. Rukhlova, A. Hadjizadeh, M. N. Bureau, *J. Biomed. Mater. Res. Part B: Appl. Biomater.* **2011**, 97B, 201.
- [8] Z. W. Ma, M. Kotaki, T. Yong, W. He, S. Ramakrishna, *Biomaterials* **2005**, 26, 2527.
- [9] P. H. Bilsen, G. Krenning, D. Billy, J. L. Duval, J. H. Vincent, M. J. Luyn, *Colloids Surf., B* **2008**, 67, 46.
- [10] Y. Marois, N. Chakf, R. Guidoin, R. C. Duharnelt, R. Roy, M. Marois, M. W. King, Y. Douville, *Biomaterials* **1996**, 17, 3.
- [11] G. Koromilaa, G. P. Michanetzi, Y. F. Missirlis, S. G. Antimisiaris, *Biomaterials* **2006**, 27, 2525.
- [12] E. I. Lev, A. R. Assali, I. Teplisky, E. Rechavia, D. Hasdai, O. Sela, N. Shor, A. Battler, R. Kornowski, *Am. J. Cardiol.* **2004**, 93, 741.
- [13] T. Magoshi, H. Ziani-Cherif, S. Ohya, *Langmuir* **2002**, 18, 4862.
- [14] A. Doliska, S. Strnad, J. Stana, E. Martinelli, V. Ribitsch, K. Stana-Kleinschek, *J. Biomater. Sci., Polym. E.* **2012**, 23, 697.
- [15] H. Fasl, J. Stana, D. Stropnik, S. Strnad, K. Stana-Kleinschek, V. Ribitsch, *Biomacromolecules* **2010**, 11, 377.
- [16] H. T. Sasmazel, S. Manolache, M. Gumusderelioglu, *Plasma Processes Polym.* **2010**, 7, 588.
- [17] K. N. Pandiyaraj, V. Selvarajan, Y. H. Rhee, H. W. Kim, S. I. Shah, *Mater. Sci. Eng. C* **2009**, 29, 796.
- [18] L. N. Boi, M. Thompson, N. B. McKeown, A. D. Romaschin, P. G. Kalman, *Analyst* **1993**, 118, 463.
- [19] S. Noel, B. Liberelle, L. Robitaille, D. G. Crescenzo, *Bioconjugate Chem.* **2011**, 22, 1690.
- [20] M. S. Ellison, L. D. Fisher, K. W. Alger, S. H. Zeronian, *J. Appl. Polym. Sci.* **1982**, 27, 247.
- [21] I. Junkar, A. Vesel, U. Cvelbar, M. Mozetic, S. Strnad, *Vacuum* **2010**, 84, 83.
- [22] K. Fukatsu, *J. Appl. Polym. Sci.* **1992**, 45, 2037.
- [23] Y. X. Liu, T. He, C. Y. Gao, *Colloids Surf. B Biointerfaces* **2005**, 46, 117.
- [24] A. Vesel, I. Junkar, U. Cvelbar, J. Kovac, M. Mozetic, *Surf. Interface Anal.* **2008**, 40, 1444.
- [25] S. Liu, N. Zhao, S. Rudenja, *Macromol. Chem. Phys.* **2010**, 211, 286.
- [26] N. Zhao, S. Liu, *Eur. Polym. J.* **2011**, 47, 1654.
- [27] L. D. Li, N. Zhao, S. Liu, *Polymer* **2012**, 53, 67.
- [28] Y. H. Wei, P. J. Wesson, I. Kourkine, B. A. Grzybowski, *Anal. Chem.* **2010**, 82, 8780.
- [29] U. Sakee, C. Nasuk, *Carbohydr. Res.* **2010**, 345, 1222.
- [30] G. C. Steffens, C. Yao, P. Prével, M. Markowicz, P. Schenck, E. M. Noah, N. Pallua, *Tissue Eng.* **2004**, 10, 1502.
- [31] P. H. Weigel, T. G. Paul, *Biomaterials* **2003**, 24, 3989.
- [32] C. H. Jou, L. Yuan, S. M. Lin, M. C. Hwang, W. L. Chou, D. G. Yu, C. Y. Ming, *J. Appl. Polym. Sci.* **2007**, 104, 220.
- [33] P. K. Smith, A. K. Mallia, G. T. Hermanson, *Anal. Biochem.* **1980**, 109, 466.
- [34] I. K. Kang, O. H. Kwon, Y. M. Lee, Y. K. Sung, *Biomaterials* **1996**, 17, 841.
- [35] M. C. Yang, W. C. Lin, *J. Polym. Res.* **2002**, 9, 201.
- [36] W. C. Lin, C. H. Tseng, M. C. Yang, *Macromol. Biosci.* **2005**, 5, 1013.
- [37] S. Dimitrievska, M. Maire, G. A. Diaz-Quijada, L. Robitaille, A. Ajji, L. Yahia, M. Moreno, Y. Merhi, M. N. Bureau, *Macromol. Biosci.* **2005**, 11, 493.
- [38] G. Rodriguez, M. Fernandez-Gutierrez, J. Parra, A. Lopez-Bravo, N. G. Honduvilla, J. Bujan, M. Molina, L. Duocastella, J. Roman, *Biomacromolecules* **2010**, 11, 2740.
- [39] W. C. Lin, T. Y. Liu, M. C. Yang, *Biomaterials* **2004**, 25, 1947.
- [40] J. Li, X. J. Huang, J. Ji, P. Lan, J. Vienken, T. Groth, Z. K. Xu, *Macromol. Biosci.* **2011**, 11, 1218.
- [41] J. Andersson, J. Sanchez, K. N. Ekdahl, G. Elgue, B. Nilsson, R. Larsson, *J. Biomed. Mater. Res.* **2003**, 67A, 458.
- [42] R. D. Rosenberg, P. S. Damus, *J. Biol. Chem.* **1973**, 248, 6490.
- [43] J. H. Ke, M. F. Wei, M. J. Shieh, T. H. Young, *J. Biomater. Sci.* **2011**, 22, 1215.
- [44] D. K. Han, K. D. Park, K. D. Ahn, S. Y. Jeong, Y. H. Kim, *J. Biomed. Mater. Res. A1* **1989**, 23, 87.